Time-Harmonic Modeling of Squirrel-Cage Induction Motors: A Circuit-Field Coupled Approach

R. Escarela-Perez[1,*], E. Melgoza[2] and E. Campero-Littlewood[1]
[1]Universidad Autonoma Metropolitana - Azcapotzalco, Departamento de Energia, Av. San Pablo 180, Col. Reynosa, C.P. 02200, Mexico D.F., MEXICO, [2]Instituto Tecnologico de Morelia, Av. Tecnologico 1500, Morelia, Mich., C.P. 58120, MEXICO.
*Corresponding author: Av. Cuauhtemoc 963, Depto 404A, Col. Narvarte Poniente, Mexico, D.F., MEXICO, r.escarela@ieee.org

Abstract: Finite element modeling of three-phase induction machines requires the solution of coupled circuit and field equations. This work aims to solve this problem using a strong coupling approach. The machine stator is fed through a three-phase non-ideal voltage source and the end winding effects are accounted for with inductances and resistances. The bars of the double squirrel cage of the rotor are modeled as solid conductors and interconnected through end-ring sections that have finite impedance. Since steady-state is considered, a time-harmonic approach has been used to perform the machine simulations.

Keywords: Induction machines, Circuit-field Coupling, 2D finite-element analysis.

1. Introduction

The accurate modeling of induction machines requires precise representation of geometry, material properties and excitations. Current-fed modeling can be readily achieved with classical finite element formulations. However, squirrel-cage asynchronous machines are voltage fed at the stator terminals through external impedances and a voltage source. In addition, the rotor has a rather complicated arrangement of bars, which are short-circuited with end-rings of finite impedances, that needs to be considered. This leads to a coupled problem where field and circuit variables must be solved together. There are basically two approaches to achieve this goal: a) simultaneous solution of both systems of equations (strong coupling) and b) field and circuit systems are solved independently, using their respective solutions to excite each separate system (weak coupling). The theory for strong coupling of field and circuit systems can be found for instance in references [1-5]. Published examples of weak coupling approaches are given in [6-8]. Neglecting the external circuit connections can lead to important errors in the prediction of the machine torque and currents. Other difficulty when dealing with induction machines is the small air-gap that requires special attention while obtaining a proper meshing of this domain. This work addresses these problems, namely circuit field coupling and proper air-gap meshing, using the AC/DC module of COMSOL Multiphysics. As a result, a quasi-3D model can be obtained with accurate representation of overhang effects and coupling with external circuits. Solid and filamentary conductors are properly accounted for. The modeling of rotor and stator with meshes of different density is also presented along with the incorporation of rotor motion through modification of rotor conductivities and resistances ("slip referring" to stator frequency). Antiperiodic boundary conditions are considered in this work to reduce the size of the final numerical model. Comparison of the full model againts models neglecting coupling with external circuits and overhang effects clearly shows the importance of considering quasi-3D models. A brief discussion about the use of time-harmonic models in the determination of initial conditions required by transient models is also given. Finally, the manuscript shows the calculation of the torque-slip curve implemented with the aid of COMSOL's Maxwell stress implementation.

2. Magnetic Field Equations

The Maxwell's equations that fully describe the modeling of low-frequency electromagnetic devices in two dimensions are

$$\begin{aligned} \nabla \times E &= -\frac{\partial B}{\partial t} \\ \nabla \cdot B &= 0 \\ \nabla \times H &= J \end{aligned} \qquad (1)$$

where the displacement current and free charges have been disregarded. E, B, $H \in \mathbb{R}^2$ are the electric field, the magnetic flux density and the magnetic field, respectively. They are strictly contained in a plane. $J \in \mathbb{R}$ is the current density and its direction is perpendicular to the plane of E, B and H. The equations (1) can be combined to give the following diffusion-type equation

$$\begin{aligned} &\sigma\frac{\partial A}{\partial t}+\nabla\times(\frac{1}{\mu_0\mu_r}\nabla\times A) \\ &-\sigma v\times(\nabla\times A)=\frac{\sigma\Delta V}{d}+J^e \end{aligned} \tag{2}$$

with $B=\nabla\times A$, where $A \in \mathbb{R}$ is the magnetic vector potential and is parallel to J, $\mu_0 \in \mathbb{R}$ is the magnetic permeability of vacuum and $\mu_r \in \mathbb{R}$ is the relative permeability. $J^e \in \mathbb{R}$ is an external current density imposed in conductor regions and it is also parallel to J. It is uniform at the conductor cross section. This current density is usually unknown since its value depends on the magnetic vector potential and the external elements connected to the conductor. Conductors have length $d \in \mathbb{R}$ with a potential difference $\Delta V \in \mathbb{R}$ which is usually unknown as well. $v \in \mathbb{R}^2$ is a velocity term that may account for moving conductors in problems where the same geometry is preserved as the conductor changes position. Analytical solution of (2) is difficult or impossible for rotating electrical machines due to their intricate geometries, proper consideration of material properties and external elements interacting with them. Numerical approximations are normally employed and the Finite Element Method [9] is widely used to obtain high quality solutions. If the static regions and the moving conductors are each modeled in their own reference frames (motion is explicitly modeled), the velocity term can be dropped out as follows

$$\sigma\frac{\partial A}{\partial t}+\nabla\times(\frac{1}{\mu_0\mu_r}\nabla\times A)=\frac{\sigma\Delta V}{d}+J^e \tag{3}$$

2.1 Time-harmonic representation

If all magnetic and electric quantities have sinusoidal variation with an electrical angular speed $\omega \in \mathbb{R}$, they can be conveniently represented in the frequency domain using the classical phasor concept of circuit theory. This way, E, B, $H \in \mathbb{C}^2$ and J, $\Delta V \in \mathbb{C}$ are now complex quantities whereas $\partial/\partial t$ is substituted by $j\omega$. Equation (2) can then be rewritten as

$$\begin{aligned} &j\omega\sigma A+\nabla\times(\frac{1}{\mu_0\mu_r}\nabla\times A) \\ &-\sigma v\times(\nabla\times A)=\frac{\sigma\Delta V}{d}+J^e \end{aligned} \tag{4}$$

3. Induction machine basics

The stator currents of three-phase induction machines operating under balanced and steady state conditions produce a magnetic field that rotates at synchronous speed $\omega_s \in \mathbb{R}$. $\omega_s = \omega$ for two-pole machines. The rotor of an induction machine moves with a speed $\omega_r \in \mathbb{R}$ that differs from the synchronous speed and therefore voltages and currents are induced in the rotor circuits. The speed difference can be calculated as $s\omega_s$, where $s \in \mathbb{R}$ is known as the rotor slip. Thus, the rotor currents produce a magnetic field rotating at this slip speed with respect to the rotor, which in turn is moving at velocity $(1\text{-}s)\omega_s$. As a result, the magnetic field of the rotor currents rotates at the same speed of the stator field. The interaction of these two magnetic fields produces an electromagnetic torque.

If the machine is excited with sinusoidal quantities, it is possible to have a static geometry in the frequency domain. This implies that slot effects are disregarded, but this effect can be reduced by positioning the rotor in a location where the electrical quantities have their average value over an electrical cycle. The frequency of the voltages and currents in the rotor conductors differs from the frequency $f \in \mathbb{R}$ in the stator conductors. The rotor frequency is proportional to the slip (sf) and this must be reflected in the machine modeling. In standard electrical machine theory this is achieved by using an equivalent circuit where the rotor impedance is a slip function. The representation of induction machines with (4) must acknowledge this fact. There are two ways to achieve this goal. One involves using the classical concepts of electrical machine theory and the other one involves the manipulation of the velocity term in (2) (see below).

3.1 Stator field equations

It is convenient to divide the machine in two sub-domains: stator and rotor. The stator domain contains the stator core, the phase conductors and part of the air gap. The rotor domain contains the rotor core, the rotor conductors and the remaining part of the air gap. The stator winding conductors can usually be considered with negligible eddy-current effects (filamentary conductors) since the dimensions of their cross sections are comparable with the skin depth at power frequency. Thus, the stator can be represented with the following set of equations

$$\begin{aligned} \nabla\times(\frac{1}{\mu_0}\nabla\times A) &= J^e \\ \nabla\times(\frac{1}{\mu_0}\nabla\times A) &= 0 \\ \nabla\times(\frac{1}{\mu_0\mu_r}\nabla\times A) &= 0 \end{aligned} \qquad (5)$$

The first equation applies to stator conductor regions. Air is represented with the second equation while iron core is described by the third equation. A and J^e vary with rated frequency.

3.2 Rotor field equations

The conductors of squirrel cage type rotors must consider the eddy current effect. Hence, the set of equations for the rotor domain are given by

$$\begin{aligned} j\omega\sigma(s)A+\nabla\times(\frac{1}{\mu_0}\nabla\times A) &= \frac{\sigma(s)\Delta V}{d} \\ \nabla\times(\frac{1}{\mu_0}\nabla\times A) &= 0 \\ \nabla\times(\frac{1}{\mu_0\mu_r}\nabla\times A) &= 0 \end{aligned} \qquad (6)$$

where the conductivity is a function of s. Actually $\sigma(s)$ is proportional to the actual rotor bar conductivity ($\sigma(s)= s\sigma$) and refers the rotor quantities to the stator frequency. This procedure is fully equivalent to the derivation of the equivalent circuit of induction machines in classical electrical machine theory where the rotor resistance is divided by s [10]. An equivalent way of getting this result is by manipulating the $\sigma v\times(\nabla\times A)$ term as shown in [11] with space and time phasors.

4. External circuit conditions

External conditions that cannot be directly included within the field model must be incorporated in order to properly predict the machine operation. The stator is connected to a three-phase voltage source through the end-winding impedance. Figure 1 shows the interconnection of the field and stator circuit model.

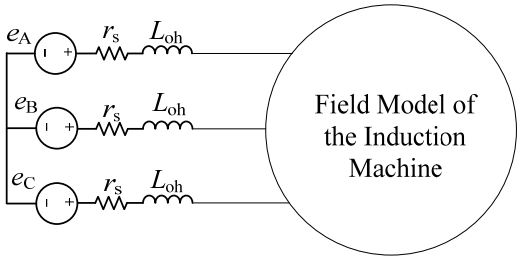

Figure 1. Voltage source feeding the induction machine. $r_s \in \mathbb{R}$ is the source resistance while $L_{oh} \in \mathbb{R}$ is the end-winding inductance of the stator windings.

The rotor conductors are also interconnected through external impedances. For a squirrel cage rotor, the conductors are solid and short-circuited through conducting end rings of finite impedance. The equivalent circuit of the rotor circuit is shown in Figure 2. The squirrel cage bars are represented by gray rectangles and they belong to the field domain. The shown resistances $r_{er} \in \mathbb{R}$ have all the same value and account for the end-ring sections that interconnect the cage bars. Likewise, the inductances of the cage circuit $L_{er} \in \mathbb{R}$ have all the same value.

The end-ring resistances must be divided by s, just as in the equivalent circuit of induction machines, for correct representation of the rotor impedance at stator frequency. Notice that the rotor circuit shown in Figure 2 accounts for the anti-periodic boundary conditions of the machine. Only one pole pitch is required to represent the whole machine behavior.

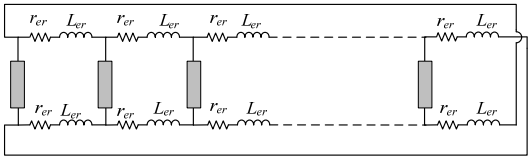

Figure 2. Squirrel cage equivalent circuit with cage bars represented by the field model. r_{er} and L_{er} are the resistance and inductance of the end-ring section connecting two cage bars.

5. Current and voltage relationships

The coupling of circuit and field variables requires explicit expressions for the voltages in all machine conductors. The voltage expression for filamentary conductors is easily obtained from Faraday's law and the voltage drop caused by the filamentary conductor resistance:

$$e = ir + Ndj\omega A \tag{7}$$

where $N \in \mathbb{Z}$ is considered the number of series-connected conductors in a given cross section and $j\omega NA$ the conductor flux linkages per unit depth. i is the circulating current in each filamentary conductor. The current density of the N filamentary conductors is given by

$$J^e = \frac{Ni}{S} \tag{8}$$

where S is the area occupied by the N series-connected filamentary conductors.

The total current circulating through a solid conductor can be found by integrating $j\omega\sigma(s)A$ and $\frac{\sigma(s)\Delta V}{L}$ from the first equation of (6) over the conductor cross section:

$$i_{sol} = \int\left(\frac{s\sigma\Delta V}{L} - js\omega\sigma A\right)d\Omega \tag{9}$$

Solving for ΔV gives

$$\Delta V = r_{sol}\left(i_{sol} + js\omega\sigma\int A d\Omega\right) \tag{10}$$

where r_{sol} is the dc resistance of the solid conductor (the resistance of the conductor at zero frequency). Equations (7)–(10) couple the field model with the exterior circuit system.

6. Numerical model and results

The induction machine considered in this work is a double squirrel cage induction motor. It is a two-pole, 7.5 kW, 380 V, 50 Hz, three-phase star connected motor. Its geometry is depicted in figure 3 and its finite-element mesh is shown in figure 4. Lagrange-quadratic elements were use to perform the numerical simulations. Two independent meshes were first constructed: one for the stator domain and another for the rotor region (see sub-sections 3.1 and 3.2). They were stitched together using the "create pairs" capability of COMSOL. The "perpendicular induction currents, vector potential application" mode of the AC/DC module of COMSOL includes the field equations presented in section 3, allowing the proper specification of material properties and boundary conditions. The machine also offers anti-periodic boundary conditions which means that:

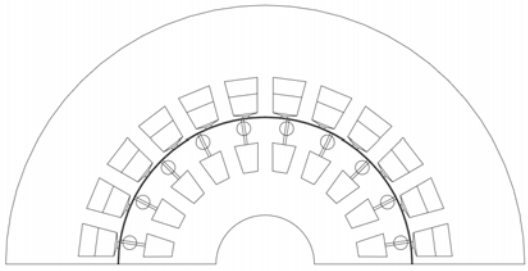

Figure 3. Machine geometry.

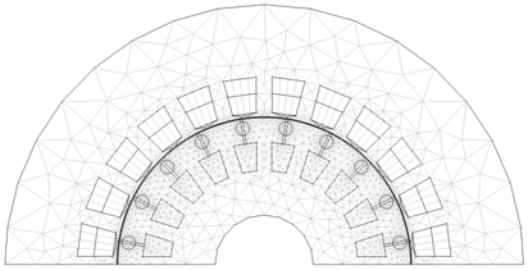

Figure 4. Finite-element mesh.

$$A(r,\theta) = A(r,\theta)e^{j180^0} \tag{11}$$

for the two-machine pole considered in this work.

Equations (7) and (10) can be readily computed using integration coupling variables at appropriate sub-domains. The resultant values of the integration coupling variables are inputted as a potential ΔV difference inout in the sub-domain settings of the rotor bars. Likewise, equation (8) is calculated as a global scalar expression that is later used as a sub-domain setting of stator conductor sub-domains. Hence, the COMSOL interface with SPICE circuit lists becomes available and the problem is fully set up.

Figure 5 shows the flux plot for rated operating conditions. It can be seen that the magnetic field can penetrate well into the rotor core because the slip is small and the effective rotor conductivity reflects this fact ($\sigma(s)= s\sigma$). Figure 6 shows the flux plot for the locked-rotor operating condition with rated voltage and frequency applied at the stator terminals. In this case, the effective rotor conductivity equals the actual conductivity of the rotor bars. Now, it can be observed that the magnetic field is only reaching the outer parts of the rotor body due to the stronger eddy current effects in the squirrel cage.

A parametric analysis can be easily performed by allowing the slip to vary from 0 to 1 (motor operation). The electromagnetic torque for each slip is computed using the Maxwell stress tensor. These results are depicted in figure 7, where the expected behavior of the electromagnetic torque versus slip is readily seen.

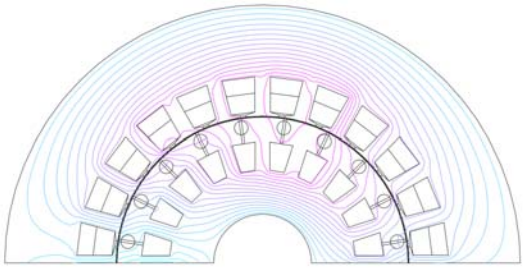

Figure 5. Rated Operating Condition.

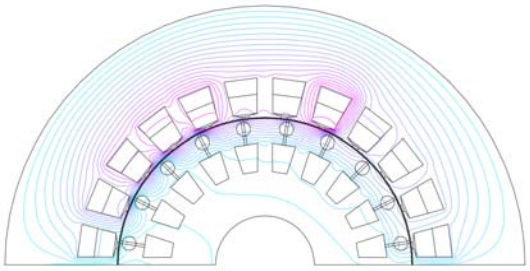

Figure 6. Rotor at standstill and rated voltage and frequency applied at the stator terminals.

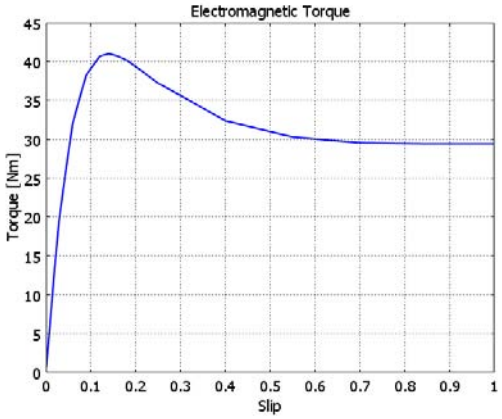

Figure 7. Electromagnetic torque versus slip.

Transient simulations of induction machines are important to predict non steady-state operating conditions. The determination of initial conditions is important for accurate transient computation. This means that in most cases an additional transient simulation is required. Computational savings can be obtained by using time-harmonic solutions since the actual solution would be near them. The time-harmonic solution is not the exact initial condition because tooth harmonics and non-linearity have not been taken into account.

Finally, it is important to emphasize that neglecting the overhang effects, such as the end-ring impedances, leads to large errors. This is shown with the calculated current at rated operating conditions. A value of 8.74 A is obtained when the end-ring impedances are considered while 12.67 A is found when they are diregarded. This implies a 45% error which cannot be neglected, and stresses the need of

quasi-3D models such as the one presented in this work.

7. Conclusions

Time harmonic modeling of induction machines is important for predicting their steady-state operation. Ferromagnetic materials can only be considered linear at the moment with COMSOL or using a rather complicated procedure to find an equivalent complex permeability. It has been found that interconnection of external systems to the field model is important to avoid large errors. Correct identification of solid and filamentary conductors must be carried out to avoid large problems and to properly model eddy current effects. The capacity of COMSOL for stitching two meshes of different densities provides a convenient way of forming quality meshes at the air gap regions.

8. References

1. P. Lombard and G. Meunier, A general purpose method for electric and magnetic combined problems for 2D, axisymmetric and transient systems, *IEEE Trans. on Magnetics*, **29(2)**, 1737–1740 (1993)
2. J. R. Brauer, B. E. MacNeal, L. A. Larkin, and V. D. Overbye, New method of modeling electronic circuits coupled with 3D electromagnetic finite element models, *IEEE Trans. on Magnetics*, **27(5)**, 4085–4088 (1991).
3. S. J. Salon, M. J. DeBortoli, and R. Palma, Coupling of transient fields, circuits, and motion using finite element analysis, *Journal of Electromagnetic Waves and Applications*, **4(11)**, 1077–1106 (1990).
4. H. De Gersem, K. Hameyer, and T. Weiland, Field-circuit coupled models in electromagnetic simulation, *Journal of Computational and Applied Mathematics*, **168(1-2)**, 125–133 (2004).
5. P. Zhou, W. N. Fu, D. Lin, S. Stanton, and Z. J. Cendes, Numerical modeling of magnetic devices, IEEE Trans. on Magnetics, **40(4)**, 1803–1809 (2004)
6. G. Bedrosian, A new method for coupling finite element field solutions with external circuits and kinematics, *IEEE Trans. on Magnetics*, **29(2)**, 1664–1668 (1993)
7. P. Zhou, D. Lin, W. N. Fu, B. Ionescu, and Z. J. Cendes, A general cosimulation approach for coupled field-circuit problems, *IEEE Trans. on Magnetics*, **42(4)**, 1051–1054 (2006).
8. E. Lange, F. Henrotte, and K. Hameyer, A circuit coupling method based on a temporary linearization of the energy balance of the finite element model, *IEEE Trans. on Magnetics*, **44(6)**, 838–841 (2008).
9. J. P. A. Bastos and N. Sadowski, *Electromagnetic Modeling by Finite Element Methods*. Marcel Dekker Inc. (2003).
10. A. E. Fitzgerald, C. K. Kingsley and S. D. Umans, *Electric Machinery*. Mc Graw Hill. (2003).
11. N. Bianchi, *Electrical Machine Analysis using Finite Elements*. CRC Press, Taylor & Francis Group. (2005).

9. Acknowledgements

This work was supported in part by the National Council of Science and Technology (CONACYT-MEXICO) and in part by the National System of Researchers (SNI-MEXICO).